TRIANGULATION AND SELF-CALIBRATION OF ADS40 IMAGERY: A CASE STUDY OVER THE PAVIA TEST SITE

V. CASELLA[1], M. FRANZINI[1], S. KOCAMAN[2], A. GRUEN[2]
[1] Geomatics Laboratory, DIET, University of Pavia
Via Ferrata, 1, I - 27100 Pavia, Italy
<vittorio.casella><marica.franzini>@unipv.it
[2] Institute of Geodesy and Photogrammetry, ETH Zurich
ETH-Hoenggerberg, CH-8093 Zurich, Switzerland
<skocaman><agruen>@geod.baug.ethz.ch

KEY WORDS: Airborne, Three-Line-Scanner, pushbroom, triangulation, self-calibration.

ABSTRACT
The particular sensor geometry of the airborne Three-Line-Scanner (TLS) requires new approaches to solve the triangulation problem. A modified bundle adjustment algorithm with the possibility of using three different trajectory models and self-calibration has been developed at the Institute of Geodesy and Photogrammetry (IGP), ETH Zurich and implemented in the TLS software.
The ADS40 camera is a commercial example of the airborne TLS. The software package, called Orima, distributed by the product vendor, Leica Geosystems AG, Heerbrugg includes specialized tools for the triangulation of the ADS40 images. The triangulation algorithm implemented in the Orima models the flight trajectory and provides self-calibration capability.
3 image strips taken at 2000 m flight altitude over the Pavia Test Site, Italy, have been processed by the research groups at the Geomatics Laboratory, University of Pavia and at the IGP, ETH Zurich. The main aim of this study is to investigate the geometric accuracy of the ADS40 camera under several GCP distributions and to compare the different processing methods used by both groups. The triangulation procedures are performed using the TLS Software at the IGP Group and the Orima Software at the Pavia Group.
The tests are performed with different numbers and distributions of GCPs and with and without self-calibration. In addition, two of the trajectory models are tested at the IGP. The test results are evaluated in terms of internal precision and external accuracy. The accuracy assessment procedure is based on the statistical parameters, which are obtained from the analysis of the covariance matrix of system unknowns and the residuals of the checkpoint ground coordinates.

1 INTRODUCTION

1.1 Background

The introduction of digital line sensors into the field of aerial photogrammetry has provided a challenging research area for photogrammetrists due to its fairly new sensor geometry and wide-range of spectral data availability. Cameras based on linear CCD sensors like the Wide Angle Airborne Camera WAAC (Boerner et al., 1997), the High Resolution Stereo Camera HRSC (Wewel et al., 1999), the Digital Photogrammetric Assembly DPA (Haala et al., 1998) were the first digital systems being used for airborne applications. The first commercial line scanner Airborne Digital Sensor ADS40 was developed by LH Systems jointly with DLR (Reulke et al., 2000, Sandau et al., 2000). In the year 2000, Starlabo Corporation, Tokyo designed the airborne Three-Line-Scanner (TLS) system, jointly with the Institute of Industrial Science, University of Tokyo (Murai and Matsumoto, 2000). The system was lately called STARIMAGER.

The ETH Zurich approach to the triangulation problem employs different trajectory models. A modified bundle adjustment algorithm based on the collinearity equation has been developed at the Institute of Geodesy and Photogrammetry (IGP), ETH Zurich. Three different types of trajectory models have already been addressed by Gruen and Zhang (2003): (a) Direct georeferencing model with stochastic exterior orientations (DGR), (b) Piecewise Polynomials with kinematic model up to second order and stochastic first and second order constraints (PPM) and (c) Lagrange Polynomials with variable orientation fixes (LIM). These models are used for the improvement of the exterior orientation parameters, which are measured by the GPS and the INS systems. A number of ground control points are needed for this approach in order to achieve high accuracies. In addition, self-calibration capability is added to the sensor model using 18 additional parameters to model the systematic errors of the camera. Detailed explanations on the additional parameters and their use in two different testfields can be found in Kocaman et al. (2006).
The Orima approach to the triangulation problem uses the orientation fixes concept. The algorithmic details are given in Hinsken et al. (2002). When compared to the LIM of the IGP, the models are similar in terms of estimating the exterior orientation parameters (EOP) at the orientation fixes. A self-calibration model, originally developed for frame cameras, was adapted for the ADS40 sensor and is currently available in Orima (Tempelmann et al., 2003).

1.2 The dataset

In August 2004 three ADS40 photogrammetric blocks, with different flying heights (2000, 4000 and 6000 m), were acquired over the Pavia Test Site (PTS) by the Italian company CGR. Seven East-West strips were taken: two for the 6000 m flying height, two for the 4000 m one and three for the 2000 m height. The staggered-array functionality was switched off, so that only one line was acquired for the backward and forward views.
In the present paper only the 2000 m flying height will be considered. The average ground resolution for this flight is ~20 cm. Figure 1 shows the strip outlines of the considered flight in red. The blue rectangle represents the area where the triangulation is performed.

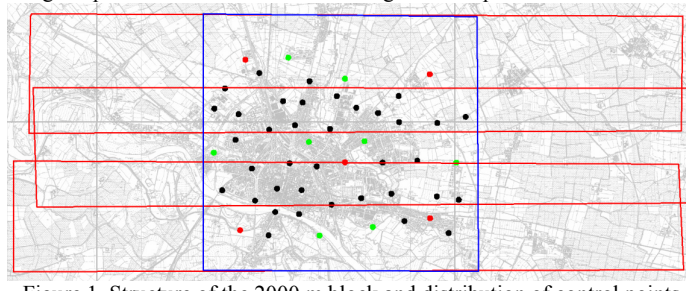

Figure 1. Structure of the 2000 m block and distribution of control points.

Figure 1 also shows the control points used, having a size of 60 cm, with a colour code: the red ones are used as control points when the 5 GCP configuration is considered; when the 12 GCP configuration is assessed, instead, the four red corner points plus the green ones are used; black points are uniquely used as independent check points, for accuracy assessment.

2 METHODOLOGY

2.1 Camera and trajectory model: the ETH Zurich approach

Three trajectory models have been implemented by Gruen and Zhang (2003) for the triangulation of the TLS sensors. However, only two of them, the DGR and the LIM, are tested within this study.

The DGR models the systematic errors of the image trajectory as a whole. 3 positional shift, 3 attitude shift and 3 attitude drift parameters are employed in the model. With the LIM, the exterior orientation parameters are determined in the so-called orientation fixes, which are introduced at certain time intervals. Between the orientation fixes, the exterior orientation parameters of an arbitrary scan line are interpolated using Lagrange polynomials. This method has been developed by Ebner et al. (1992) for orientation of MOMS images, and modified by Gruen and Zhang (2003) according to the TLS sensor model with the provision of auxiliary position/attitude data generated by the GPS/INS system.
Chen et al. (2003) described the CCD line structure and calibration of the TLS camera. Starting from this point, a total of 18 additional parameters (APs) are identified, implemented, and tested at the IGP, ETH Zurich. The AP set consists of:

- Δc: Systematic error in the focal length of the camera lens.
- Δx_{pb}, Δx_{pn}, Δx_{pf}: Displacements of the line centers of the three Linear Array CCDs from the principle point (PP) of the camera lens, defined in the flight direction.
- Δy_{pb}, Δy_{pn}, Δy_{pf}: Displacements of the line centers of the three Linear Array CCDs from the principle point (PP) of the camera lens, defined across the flight direction.
- *Lens Distortion Parameters:* Radial symmetric lens distortion (k_1, k_2, k_3) and decentering distortion (p_1, p_2) models of Brown (1971).
- s_{yb}, s_{yn}, s_{yf}: Affinity is defined in x direction by Beyer (1992) for close-range frame CCD cameras. In this study, affinity parameters for each CCD line are used in the (y) direction.
- $\Delta\theta_b$,$\Delta\theta_n$, $\Delta\theta_f$: The $\Delta\theta$ parameters represent the systematic errors of the inclination angle between each CCD line and the (y) axis of the camera coordinate system.

The self-calibration algorithm presented here aims to determine the optimal set of APs for the optimal estimation of the object space coordinates of the measured image points. The adjustment procedure starts with the full parameter set and eliminates undeterminable parameters automatically in an iterative approach. The APs are introduced as free unknowns into the system. The major problem for parameter elimination is the finding of robust criteria for rejection of undeterminable parameters. A stepwise parameter elimination algorithm proposed by Gruen (1985) is used here. The APs are described in more detail in Kocaman et al. (2006).

2.2 Camera and trajectory model: the University of Pavia approach

The Pavia group used the commercial software supplied by the ADS40 camera vendor: Socet Set 4.4.1, Gpro 2.1 and Orima 6.1; it is the same configuration used by the CGR company which supplied the data.
An image coordinate system is defined on the focal plane of the camera: the origin coincides with the principal point, the x-axis is parallel to the flight direction, and y-axis is parallel to the sensor lines. The theoretical camera model assumes that sensor lines are parallel to the y-axis and occupy the nominal positions. They are linear and planar. The CCD elements are equally spaced and the lens is undistorted.
In-flight camera calibration is performed by the manufacturer and deviations from the theoretical model, caused by lens distortion, offset and inclination of sensor lines, are quantified. A mathematical model of deviations is estimated and then calibration files are written. They contain, for every sensor line, a look up table with the image coordinates of the centre of each CCD element: these coordinates are determined in order to compensate for any camera deviation. The conversion between the pixel coordinates and the image coordinates of a certain feature is performed through the look up tables therefore the obtained pixel coordinates are virtually free of any distortion. In this paper, the basic camera model refers to the theoretical one integrated with the calibrated look up tables.
With the Orima software, it is possible to estimate a 7-parameter datum transformation in the case that GPS/IMU and GCP data relate to different reference systems. The misalignments between camera and IMU reference systems can also be treated as unknowns. In addition, a self-calibration

method, which aims to improve the given calibration, can be performed. The Brown model (Brown, 1976) has been implemented in Orima: it has 21 parameters and was originally defined for large-format, analogue frame cameras, but it was adapted for line cameras too. The second camera model considered in the paper, named self, includes camera self-calibration and datum transformation parameters.
The trajectory model implemented in Socet Set and Orima is based on the orientation fixes concept. For the mathematical description of this model, please see Hinsken et al. (2002). In the bundle adjustment, the exterior orientation parameters (EOP) of predefined orientation fixes are estimated. The EOP at any time are obtained through the linear interpolation of corrections, meaning that the adjusted EOP of the fixes are used together with the original GPS/IMU observations.

3 TEST RESULTS

The triangulation and the accuracy assessment have been carried out independently by the two Groups. The stochastical model parameters and the test network configurations are arranged identically. The trajectory models are tested both with and without self-calibration.

3.1 Preparation of the test data

The image coordinate measurements of the control points are manually performed at the Geomatics Laboratory of the University of Pavia, with the programs Socet Set and Orima, and successively provided to the IGP Group. Tie points are extracted and measured automatically with the APM procedure of Socet Set. Image measurements are performed once per flight. Gross error detection procedures are performed by both Groups in turn. The final point set is used for the tests presented in this paper.
Ground coordinates of control points are measured by the Pavia group: the accuracies of the coordinates are better than 1 cm for X,Y,Z. 46 signalised control points are measured on the images. Two different GCP configurations (5 and 12 GCPs) are tested in order to quantify the effect of the number of GCPs on the results.
The stochastical model plays a key role in the adjustment. Therefore a predefined set of apriori standard deviations are used for all tests with following values:

- image coordinates: 1/3 of a pixel (= 2.2 μm)
- object coordinates of GCPs: 1.5 cm for X,Y, and 2 cm for Z
- GPS/IMU measurements: 10 cm for X,Y, and 20 cm for Z; 0.006^g for ω,φ, and 0.009^g for κ.

3.2 University of Pavia results

The dataset is tested first with the direct georeferencing method, obtained through an aerial triangulation calculation in which the GPS/IMU measurements are overweighted and consequently kept fixed. The basic and self camera models are then assessed, each with 5 or 12 GCPs. The results are given in Table 1 and also in Figure 2.
Direct georeferencing has an accuracy of 0.5 pixels in planimetry and 3 pixels in height and there is a significant bias on the Z component. Concerning integrated sensor orientation, namely the basic and self models, the aposteriori sigma0 values range between 0.35 and 0.43 pixels.
When self-calibration is not performed, the RMSE values are around 1 pixel (considering the 20 cm Ground Sampling Distance) for planimetric components and between 1.4 and 2 pixel for height: the usage of 12 GCPs instead of 5 improves results, especially for the Z component.
Self-calibration greatly enhances the RMSE values, which are around 5 cm (1/4 GSD) for planimetry and of 9 and 6 cm (between 1/2 and 1/3 GSD) for height, when 5 and 12 GCPs are used, respectively. This large improvement highlights the existence of significant systematic errors in the

system which are corrected by the self-calibration. Using 12 GCPs instead of 5 significantly improves the height accuracy.

3.3 ETH Zurich results

Initially, a forward intersection method is applied on the check points. The results are presented in Table 2.

Table 2. Forward intersection results from check points, ETH Zurich

Value	X (m)	Y (m)	Z (m)
RMSE	0.119	0.096	0.649
Mean Sigma	0.097	0.099	0.224

The DGR and the LIM are tested in two different GCP configurations (5 and 12). The self-calibration method is applied to both models for the two GCP configurations. The LIM is tested with 4 and 18 orientation fixes. The fix number 18 is chosen to match the interval of the Orima orientation fixes approximately. The fix number 4 is chosen to observe the effect of a smaller number of orientation fixes. The results of the adjustment with the 5 and the 12 GCPs configurations are given in Table 3. The aposteriori sigma naught (sigma0) values range between 0.38-0.48 pixels. The self-calibration method brings an improvement to the sigma naught values in all test configurations. The theoretical sigma values are obtained from the analysis of the covariance matrix. The sigma values improve slightly, which can be explained with the decrease of the sigma naught values in all cases.
The RMSE values show large systematic errors on the results, which are largely corrected by the self-calibration. The improvement is observed especially on the Y coordinates and the height values.
The test results with the 5 GCP configuration are demonstrated in Figure 3. When the DGR is compared with the LIM-18, the DGR produces more stable results. This implies that the given trajectory values are accurate and even a less complex model is sufficient for modelling the trajectory errors. The instability of the LIM can further be reduced by tuning the stochastical model parameters. However, overweighting the EOPs of the orientation fixes will approach the LIM model to the DGR.
The test results with the 12 GCP configuration is given in Figure 4. When compared to the 5 GCP cases, the RMSE values are improved and resulted in 4 cm in planimetry and 5 cm in height in the best case with the DGR and self-calibration. Considering the 20 cm ground sample distance, the values correspond to 0.2 and 0.25 pixels in planimetry and in height, respectively.
Even when the self-calibration is not used, 12 GCPs provided a significant improvement in the height values. However, when the 5 GCP configuration is used with self-calibration, the results are still superior to the results of the 12 GCPs case without self-calibration. The use of self-calibration is recommended in this case for a more economical solution.

4 CONCLUSIONS

The ADS40 images acquired over the Pavia testsite are processed in terms of triangulation and self-calibration by the Geomatics Laboratory, University of Pavia, and the IGP, ETH Zurich. Different trajectory models and self-calibration methods are used by the Groups.
The direct georeferencing results of both groups, which are demonstrated in Tables 1 and 2, are identical in terms of RMSEs. The differences in the standard deviations can be explained by the differences of the methods used. The IGP results are obtained by applying forward intersection on individual check points, while the University of Pavia results are obtained in a bundle adjustment.

The dataset provides a good level of accuracy, 0.5 pixels in planimetry and 3 pixels in height, even without any further processing with GCPs.

Table 1. Results for the 2000 m flight, University of Pavia

University of Pavia				*Theoretical*	*Empirical*				
Model	**GCP/ CPs**	**Sigma0 (µm)**	**Comp.**	**STD (m)**	**Min (m)**	**Max (m)**	**Mean (m)**	**STD (m)**	**RMSE (m)**
DG	0 GCP 46 CKPs	6.6	**X**	0.11	-0.18	0.19	0.02	0.12	0.12
			Y	0.11	-0.32	0.19	-0.01	0.09	0.09
			XY	0.11					0.11
			Z	0.28	-0.97	0.05	-0.56	0.32	0.64
BASIC	5 GCPs 41 CKPs	2.6	**X**	0.05	-0.42	0.51	0.09	0.22	0.24
			Y	0.05	-0.50	0.60	0.02	0.27	0.27
			XY	0.05					0.25
			Z	0.12	-0.64	-0.06	-0.36	0.15	0.39
	12 GCPs 34 CKPs	2.8	**X**	0.05	-0.43	0.05	0.04	0.21	0.22
			Y	0.05	-0.49	0.34	-0.01	0.22	0.22
			XY	0.05					0.22
			Z	0.12	-0.47	-0.06	-0.26	0.11	0.28
SELF	5 GCPs 41 CKPs	2.3	**X**	0.05	-0.10	0.15	0.02	0.05	0.06
			Y	0.05	-0.14	0.05	-0.01	0.04	0.04
			XY	0.05					0.05
			Z	0.12	-0.19	0.16	-0.03	0.08	0.09
	12 GCPs 34 CKPs	2.3	**X**	0.04	-0.14	0.11	-0.01	0.06	0.06
			Y	0.04	-0.14	0.05	-0.01	0.04	0.04
			XY	0.04					0.05
			Z	0.10	-0.13	0.17	-0.01	0.06	0.06

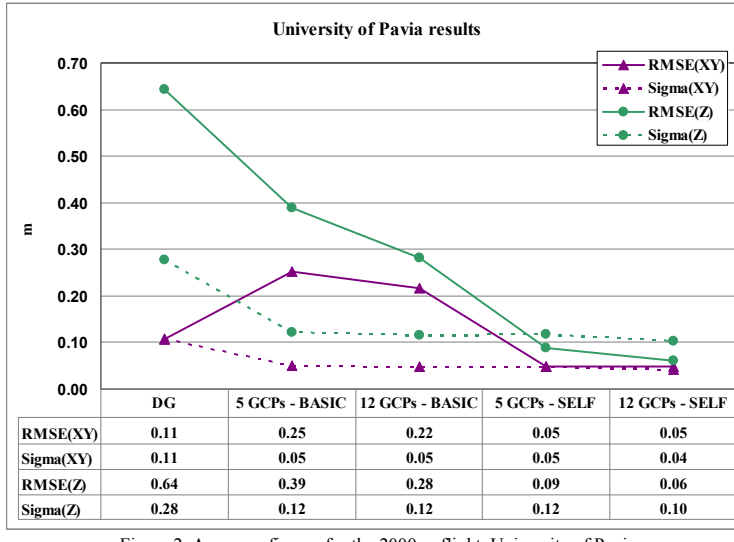

	DG	5 GCPs - BASIC	12 GCPs - BASIC	5 GCPs - SELF	12 GCPs - SELF
RMSE(XY)	0.11	0.25	0.22	0.05	0.05
Sigma(XY)	0.11	0.05	0.05	0.05	0.04
RMSE(Z)	0.64	0.39	0.28	0.09	0.06
Sigma(Z)	0.28	0.12	0.12	0.12	0.10

Figure 2. Accuracy figures for the 2000 m flight, University of Pavia

Table 3. Results for the 2000 m flight, ETH Zurich

ETH Zurich				*Theoretical*	*Empirical*				
Model	**GCP/ CPs**	**Sigma0 (µm)**	**Comp.**	**STD (m)**	**Min (m)**	**Max (m)**	**Mean (m)**	**STD (m)**	**RMSE (m)**
DGR	5 GCP 41 CP	2.96	X	0.06	-0.21	0.18	-0.05	0.08	0.10
			Y	0.06	-0.68	0.64	0.01	0.36	0.36
			XY	0.06					0.26
			Z	0.14	-0.04	0.34	0.17	0.11	0.20
DGR SC*	5 GCP 41 CP	2.57	X	0.05	-0.16	0.06	-0.06	0.06	0.08
			Y	0.05	-0.04	0.14	0.02	0.04	0.04
			XY	0.05					0.06
			Z	0.12	-0.22	0.12	-0.05	0.07	0.09
LIM-4	5 GCP 41 CP	2.88	X	0.05	-0.43	0.32	-0.09	0.18	0.20
			Y	0.06	-0.62	0.56	-0.01	0.29	0.29
			XY	0.06					0.25
			Z	0.13	-0.29	0.32	0.09	0.16	0.18
LIM-4 SC*	5 GCP 41 CP	2.55	X	0.05	-0.15	0.10	-0.04	0.05	0.06
			Y	0.06	-0.13	0.13	0.00	0.05	0.05
			XY	0.05					0.06
			Z	0.13	-0.20	0.24	0.06	0.11	0.12
LIM-18	5 GCP 41 CP	2.76	X	0.05	-0.34	0.23	-0.08	0.13	0.15
			Y	0.05	-0.69	0.58	-0.01	0.32	0.32
			XY	0.05					0.25
			Z	0.13	-0.18	0.43	0.16	0.14	0.21
LIM-18 SC*	5 GCP 41 CP	2.47	X	0.05	-0.19	0.06	-0.06	0.07	0.09
			Y	0.05	-0.27	0.22	-0.01	0.14	0.14
			XY	0.05					0.11
			Z	0.12	-0.19	0.30	0.08	0.11	0.14
DGR	12 GCP 34 CP	3.09	X	0.05	-0.22	0.25	-0.01	0.11	0.11
			Y	0.05	-0.48	0.59	0.02	0.29	0.29
			XY	0.05					0.22
			Z	0.13	-0.01	0.25	0.10	0.06	0.12
DGR SC*	12 GCP 34 CP	2.56	X	0.05	-0.14	0.15	0.00	0.05	0.05
			Y	0.05	-0.04	0.13	0.01	0.03	0.04
			XY	0.05					0.04
			Z	0.11	-0.09	0.03	-0.04	0.03	0.05
LIM-4	12 GCP 34 CP	3.02	X	0.05	-0.42	0.36	-0.03	0.18	0.18
			Y	0.05	-0.34	0.50	0.01	0.22	0.22
			XY	0.05					0.20
			Z	0.12	-0.11	0.19	0.03	0.07	0.08
LIM-4 SC*	12 GCP 34 CP	2.55	X	0.05	-0.11	0.13	0.00	0.05	0.05
			Y	0.05	-0.07	0.12	0.01	0.04	0.04
			XY	0.05					0.04
			Z	0.11	-0.12	0.09	-0.02	0.05	0.06
LIM-18	12 GCP 34 CP	2.91	X	0.05	-0.35	0.30	-0.03	0.16	0.16
			Y	0.05	-0.39	0.52	0.01	0.24	0.24
			XY	0.05					0.20
			Z	0.12	-0.15	0.27	0.05	0.09	0.10
LIM-18	12 GCP	2.47	X	0.04	-0.13	0.15	0.00	0.05	0.05

SC*	34 CP		Y	0.05	-0.15	0.14	0.01	0.08	0.08
			XY	0.04					0.07
			Z	0.11	-0.14	0.21	0.04	0.07	0.08

* SC: Self-calibration is used

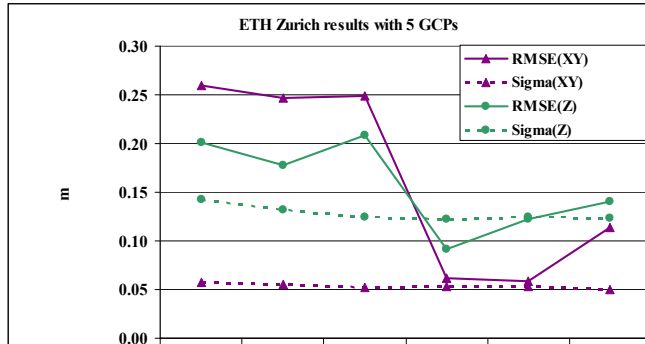

	DGR	LIM-4	LIM-18	DGR-SC	LIM-4 SC	LIM-18-SC
RMSE(XY)	0.26	0.25	0.25	0.06	0.06	0.11
Sigma(XY)	0.06	0.06	0.05	0.05	0.05	0.05
RMSE(Z)	0.20	0.18	0.21	0.09	0.12	0.14
Sigma(Z)	0.14	0.13	0.13	0.12	0.13	0.12

Figure 3. Accuracy figures for the 2000 m flight with the 5 GCP configuration, ETH Zurich

The University of Pavia approach uses the commercial software of Leica Geosystems, called Orima, for the triangulation and self-calibration. The best results are obtained with the 12 GCP configuration and by using the self-calibration. The RMSE values are 5 cm in planimetry and 6 cm in height in this case, which corresponds to 0.25 and 0.30 pixels.

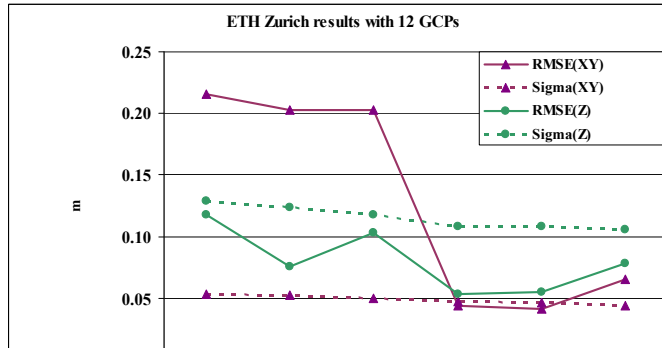

	DGR	LIM-4	LIM-18	DGR-SC	LIM-4 SC	LIM-18-SC
RMSE(XY)	0.22	0.20	0.20	0.04	0.04	0.07
Sigma(XY)	0.05	0.05	0.05	0.05	0.05	0.04
RMSE(Z)	0.12	0.08	0.10	0.05	0.06	0.08
Sigma(Z)	0.13	0.12	0.12	0.11	0.11	0.11

Figure 4. Accuracy figures for the 2000 m flight with the 12 GCP configuration, ETH Zurich

The IGP results are comparable when the self-calibration is used. The best results are obtained using the DGR model with self-calibration and the 12 GCP configuration. In this case, the RMSE values are 4 cm and 5 cm in planimetry and height, which corresponds to 0.20 and 0.25 pixels, respectively. The LIM produces slightly worse results, which could probably be controlled by tuning the statistical model elements. The use of self-calibration improves the accuracy in all cases. The use of 12 GCPs increases the overall accuracy when compared to the same test configurations with 5 GCPs.

REFERENCES

1. Beyer, H.A., 1992: Geometric and Radiometric Analysis of a CCD-Camera Based Photogrammetric Close-Range System. Dissertation, No. 9701, ETH, Zurich.
2. Boerner, A., Reulke, R., Scheele, M., Terzibaschian, Th., 1997: Stereo Processing of Image Data from an Airborne Three-Line CCD Scanner. The 3rd International Airborne Remote Sensing Conference and Exhibition, 7-10 July, Copenhagen, Denmark.
3. Brown, D.C., 1971: Close-Range Camera Calibration. Photogrammetric Engineering, 37 (8), pp. 855-866.
4. Brown, D.C., 1976: The Bundle Adjustment – Process and Prospects. Invited Paper to the XIIIth Congress of the ISPRS Comm. III, Helsinki.
5. Chen, T., Shibasaki, R., Murai, S., 2003: Development and Calibration of the Airborne Three-Line Scanner (TLS) Imaging System. ASPRS Journal of PE&RS, vol. 69, no. 1, pp. 71-78.
6. Ebner, H., Kornus, W., Ohlhof, T., 1992: A Simulation Study on Point Determination for The MOMS-02/D2 Space Project Using an Extended Functional Model. IAPRS, Washington, D. C., Vol. 29, Part B4, pp. 458-464.
7. Gruen, A., 1985: Data Processing Methods for Amateur Photographs. Photogrammetric Record, 11 (65), pp. 567-579.
8. Gruen, A., Zhang, L., 2003: Sensor Modeling for Aerial Triangulation with Three-Line-Scanner (TLS) Imagery. Journal of Photogrammetrie, Fernerkundung, Geoinformation, 2/2003, pp. 85-98.
9. Haala, N., Stallmann, D., Cramer, M., 1998: Calibration of Directly Measured Position and Attitude by Aerotriangulation of Three-Line Airborne Imagery. The International Archives of Photogrammetry and Remote Sensing, Budapest, Vol. 32, Part 3, pp. 23-30.
10. Hinsken, L., Miller, S., Tempelmann, U., Uebbing, R., Walker, S., 2002: Triangulation of LH Systems'ADS40 imagery using ORIMA GPS/IMU. Proceedings of ISPRS Commission III Symposium, on CD. 9-13 September, Graz, Austria.
11. Kocaman S., Zhang L., Gruen A., 2006: Self-calibrating Triangulation of Airborne Linear Array CCD Cameras. EuroCOW 2006 International Calibration and Orientation Workshop, Castelldefels, Spain, 25-27 Jan. (proceedings on CD-ROM).
12. Murai, S., Matsumoto, Y., 2000: The Development of Airborne Three Line Scanner with High Accuracy INS and GPS for Analysing Car Velocity Distribution. The International Archives of Photogrammetry and Remote Sensing, Amsterdam, Vol. 33, Part B2, pp. 416-421.
13. Reulke, R., Franke, K-H., Fricker, P., Pomierski, T., Sandau, R., Schoenermark, M., Tornow, C., Wiest, L., 2000: Target Related Multispectral and True Color Optimization of the Color Channels of the LH Systems ADS40. The International Archives of Photogrammetry and Remote Sensing, Amsterdam, Vol. 33, Part B1, pp. 244-250.
14. Sandau, R., Braunecker, B., Driescher, H., Eckardt, A., Hilbert, S., Hutton, J., Kirchhofer, W., Lithopoulos, E., Reulke, R., Wicki, S., 2000: Design Principle of The LH Systems ADS40 Airborne Digital Sensor. The International Archives of Photogrammetry and Remote Sensing, Amsterdam, Vol. 33, Part B1, pp. 258-265.

15. Tempelmann, U., Hinsken, L., Recke, U., 2003: ADS40 Calibration and Verification Process. Proceedings of Optical 3D Measurement Techniques Conference, Zurich, Switzerland, pp. 48-54.
16. Wewel, F., Scholten, F., Gwinner, K., 1999: High Resolution Stereo Camera (HRSC) – Multispectral Data Acquisition and Photogrammetric Data Processing. 4th International Airborne Remote Sensing Conference and Exhibition, Ottawa, Canada, Vol. I, pp. 263-272.